Rheology and Structure of a Butadiene−Styrene Diblock Copolymer in Dibutyl Phthalate: Role of Concentration Fluctuation in Disruption and Reformation of Micellar Lattice

Hiroshi Watanabe,*,† Yumi Matsumiya,† Toshiji Kanaya,† and Yoshiaki Takahashi‡

Institute for Chemical Research, Kyoto University, Uji, Kyoto 611, Japan, and Center for Integrated Research in Science and Engineering, Nagoya University, Nagoya, Aichi 464-8603, Japan

Received April 2, 2001

ABSTRACT: Rheological properties were examined for a butadiene−styrene (BS) diblock copolymer dissolved in an S-selective solvent, dibutyl phthalate (DBP). This copolymer was composed of a deuterated B block ($M_B = 13.3 \times 10^3$) and a protonated S block ($M_S = 53.9 \times 10^3$), and the microdomain structure in the quiescent state as well as under steady shear was detected with small-angle neutron scattering (SANS). At 25 °C, a quiescently equilibrated BS/DBP system of the BS concentration = 28 wt % exhibited elastic behavior under slow, small-amplitude oscillatory shear. This elasticity reflected a bcc lattice of BS micelles with B cores and S corona. Although the B cores were in the liquid state, the thermodynamic power of segregation from the S/DBP phase forced these cores to be arranged on the lattice at equilibrium. Under steady shear, the BS/DBP system exhibited significantly non-Newtonian flow behavior. At low shear rates ($\dot{\gamma}$), the steady state was attained after a significant stress overshoot followed by a thixotropic stress decay, and the viscosity η in this state was proportional to $\dot{\gamma}^{-1}$. This plastic behavior reflected mild disruption of the micellar lattice (decrease of the grain size) under slow shear. In contrast, at higher $\dot{\gamma}$, the lattice was massively disrupted to exhibit weaker $\dot{\gamma}$ dependence of η. Corresponding to this massive disruption, the BS/DBP system just after cessation of the fast pre-shear exhibited full relaxation (with no equilibrium elasticity) attributed to the B/S concentration fluctuation. This pre-sheared system reformed the micellar lattice to recover its elasticity when kept quiescently, and the slowest reformation/recovery was observed at the pre-shear rate being comparable to the frequency ω_f of the concentration fluctuation. Thus, the pre-shear at $\dot{\gamma} \cong \omega_f$ disrupted the lattice most efficiently (thereby resulting in the slowest lattice reformation). These rheological features and structures of the BS/DBP system were discussed in relation to the softness of the micellar B cores.

1. Introduction

Block copolymers exhibit a wide variety of microdomain structures in bulk state as well as in solution phases.[1−3] This structure has significant effects on both static and dynamic properties. Extensive studies have been made to elucidate these effects in various copolymer systems.[4−24]

In these studies, Watanabe et al. focused on the structure and rheological properties of styrene−butadiene (SB) and/or styrene−isoprene (SI) diblock copolymers in diene-selective solvents.[13−21] These copolymers form spherical micelles with solvated diene corona and precipitated, glassy S cores at low temperatures. These micelles form cubic lattices when their corona blocks are overlapping and osmotically interacting with each other. In the linear viscoelastic regime, this micellar lattice structure provides the system with the equilibrium elasticity (that reflects the entropic elasticity of mutually constrained corona blocks).[13−15,19,21] On screening of this osmotic interaction, the micelles are randomly dispersed to exhibit full viscoelastic relaxation (no equilibrium elasticity) that reflects orientational relaxation of individual corona blocks as well as diffusion of the micellar particles.[15,16,20] These micellar lattices and micellar dispersions also exhibit characteristic nonlinearities, damping of modulus under large step strains[17,19] and thinning of viscosity under fast flow,[18,19] according to the stress-generating mechanisms in respective systems.

In long time scales, the above rheological features of the micellar lattices are essentially the same as those of colloidal crystals having no polymeric corona.[19] The features of the micellar dispersions are very similar to those of ideal suspensions of Brownian hard spheres.[17−19] These similarities emerge because the S cores in these micellar systems are glassy and not deformed under the strain/flow examined: In long time scales, the micelles having the rigid S cores behave as the hard spheres with their effective interaction being determined by the corona blocks.

Thus, we expect that the rheological behavior of micellar systems changes and the similarities with the hard-sphere colloidal systems vanish when the micellar cores are softened. To examine this expectation, we have carried out rheological and structural measurements for a BS diblock copolymer in a moderately S-selective[22,23] solvent, dibutyl phthalate (DBP). At low temperature and high concentration, BS micelles with soft B cores and S corona were arranged on a cubic lattice to exhibit the elasticity in a quiescently equilibrated state. This micellar lattice exhibited interesting rheological and structural properties: The lattice was disrupted to various extent under steady shear at various rates, and a time required for the lattice reformation in the quiescent state was the longest when the pre-shear rate was comparable to a frequency of the B/S concentration fluctuation. In this paper, these results are described in details, and the properties of the BS/DBP micellar

* Corresponding author.
† Kyoto University.
‡ Nagoya University.

10.1021/ma0105587 CCC: $20.00
Published on Web 08/14/2001

Table 1. Characteristics of BS and BSB Copolymers[a]

code	$10^{-3}M_B$[c]	$10^{-3}M_S$[e]	M_w/M_n[f]
BS 13-54	13.3	53.9	1.03
BSB 13-108-13[b]	13.3[d]	108	1.03

[a] Composed of deuterated B and protonated S blocks. [b] Not used in this study. [c] Determined from GPC elution calibration for the precursor B block after correction of the difference of the monomer molecular weights for deuterated and protonated B. ($M_w/M_n = 1.02$ for the B block). [d] Molecular weight for each B block. [e] Evaluated from M_B of the B block and the S weight fraction in the copolymer, with the latter being determined from RI and UV signals. [f] Evaluated from GPC elution calibration for the copolymer.

system are discussed in relation to the B core softness, with the emphasis being placed on the nonlinear shear effects on the properties of the micellar lattice.

2. Experimental Section

Materials. A butadiene−styrene (BS) diblock copolymer composed of deuterated B and protonated S blocks was synthesized via living anionic polymerization in high vacuum. The initiator and solvent for the polymerization were *sec*-butyllithium and benzene, respectively. The monomers were purified with *sec*-butyllithium (for B purchased from CDN Isotopes) and with *sec*-butylmagnesium (for S from Aldrich).

In the synthesis, the B block was first polymerized, and then the S block was copolymerized. Half of the resulting BS^- anions were terminated with methanol to recover the BS sample utilized in this study. The remaining BS^- anions were coupled with 1,4-bis(chloromethyl)benzene (90% equimolar to the anions) to prepare their dimer, a BSB triblock copolymer. The crude product of this coupling reaction was thoroughly fractionated from benzene/methanol mixtures to recover the BSB sample to be utilized in our future study (not in this study).

These BS and BSB copolymers and the precursor B block were characterized with GPC (CO-8020 and DP-8020, Tosoh) equipped with refractive index/light scattering (RI/LS) and ultraviolet adsorption (UV) monitors (LS-8000 and UV-8020, Tosoh) connected in series. THF was the eluent, and previously synthesized monodisperse polybutadienes[25] were utilized as elution standards. Table 1 summarizes the characteristics of the BS and BSB samples.

The systems examined in this study were solutions of the BS sample in dibutyl phthalate (DBP). These solutions were prepared from homogeneous solutions of BS and DBP in excess methylene chloride by allowing methylene chloride to thoroughly evaporate. The BS concentration c_{BS}, determined after this evaporation, was 18, 20, 25, and 28 wt %. The reduced molecular weights at these c_{SB}, $10^{-3}\phi_{BS}M_{BS} = 11.9$, 13.2, 16.5, and 18.5 with ϕ_{BS} being the volume fraction of the BS chains (evaluated under assumption of no volume change on dissolution), were considerably smaller than the characteristic molecular weight for entanglement of S chains (the major component in the BS copolymer), $10^{-3}M_C \cong 32$.[26] Thus, the BS chains were not entangled among themselves even at the highest c_{BS} examined.

Measurements. For the BS/DBP systems with $c_{BS} = 18-28$ wt %, rheological measurements were carried out at 25 °C with a laboratory rheometer (ARES, Rheometrics). A cone-plate fixture with the plate diameter = 25.0 mm and the gap angle = 0.1 rad was used. For the 28 wt % system, the measurements were conducted also at several temperatures $T \leq 70$ °C.

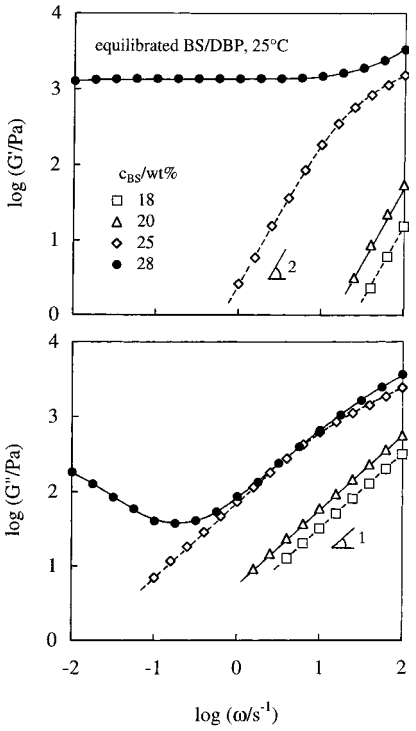

Figure 1. Linear viscoelastic behavior of the BS/DBP systems with various c_{BS} quiescently equilibrated at 25 °C. The micellar lattice is developed in the 28 wt % system to exhibit the equilibrium elasticity.

The SANS measurements were made with the SANS−U spectrometer at the Neutron Scattering Laboratory, Institute for Solid State Physics, University of Tokyo (Tokai, Ibaragi), in the following configuration: incident neutron wavelength $\lambda = 0.7$ nm, wavelength spread $\Delta\lambda/\lambda = 0.1$, sample-to-detector distance = 4.00 m, and beam diameter = 0.3 cm. The scattering intensity was measured as a function of the scattering vector **q**, where $q = |\mathbf{q}| = [4\pi/\lambda] \sin(\theta/2)$, with θ being the scattering angle.

For the 28 wt % BS/DBP system, the SANS measurements were made at 25 °C in a Couette flow cell[27] with inner and outer radii of 25.25 mm and 27.00 mm. The system was quiescently ordered in the cell (by cooling from 60 to 25 °C), and the SANS profiles were obtained before, during, and after imposition of the steady shear. The incident beam was in the direction normal to the surfaces of the inner/outer cylinders of the cell (i.e., in the direction of the velocity gradient), and the profiles were detected in a velocity−vorticity plane. All profiles, including those during/after the shear, were azimuthally symmetric. Thus, in this paper, we present the circularly averaged profiles. No correction was made for the incoherent scattering.

3. Results and Discussion

3-1. Linear Viscoelastic Behavior and Structure at Equilibrium. 3-1-1. Viscoelastic Behavior. For the BS/DBP systems with $c_{BS} = 18-28$ wt %, Figure 1 shows plots of the storage and loss moduli G' and G'' against the angular frequency ω. The BS chains are not entangled, as explained earlier. The oscillatory strain amplitude γ_0 was kept small (≤ 0.01) so that the linear responses of the structure therein were detected. Prior to the measurements, the systems charged in the rheometer were heated to 60 °C, slowly cooled to 25 °C,

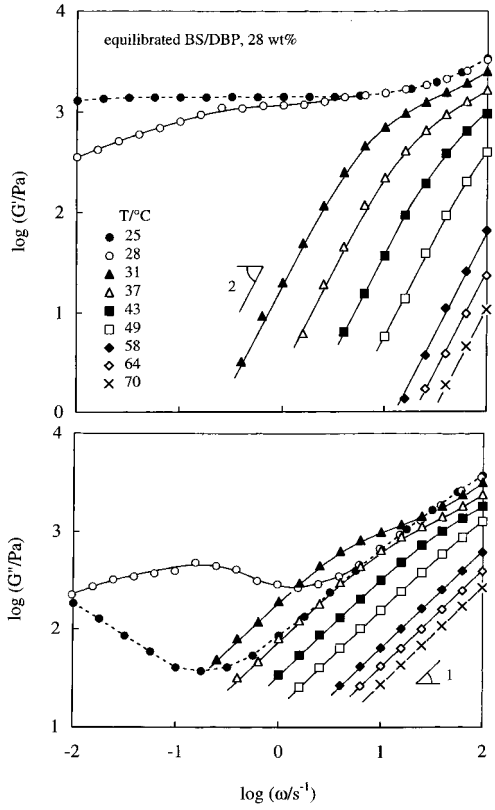

Figure 2. Linear viscoelastic behavior of the 28 wt % BS/DBP system quiescently equilibrated at various T.

and then quiescently equilibrated at 25 °C for 12 h. For all systems, the preconditioning temperature, 60 °C, was higher than the microphase-separation temperature T_{MPS}: T_{MPS} of these systems was below 58 °C, as explained in a later section examining the relaxation mechanism(s) of the 28 wt % system at $T \geq 31$ °C.

In Figure 1, fluidlike behavior characterized with the terminal tails ($G' \propto \omega^2$ and $G'' \propto \omega$) is noted for the BS/DBP systems with $c_{BS} \leq 25$ wt %. In contrast, the system with $c_{BS} = 28$ wt % exhibits elastic, solid like behavior characterized with the ω-insensitive G' ($\gg G''$) at low ω. These results indicate that the BS micelles with B cores and S corona are arranged on a cubic lattice at $c_{BS} = 28$ wt % (as confirmed later in Figure 3) and that the lattice is disordered at $c_{BS} \leq 25$ wt %. (In fact, similar rheological/structural changes with c are known for the SB micelles having glassy S cores in tetradecane.[13,14,19])

Linear viscoelastic behavior of the 28 wt % BS/DBP system was also tested at several temperatures T. In this test, the system quiescently equilibrated at 25 °C for 12 h was subjected to a stepwise increase of T from 25 to 70 °C (with an interval $\Delta T = 3$ °C), and the viscoelastic moduli (for $\gamma_0 = 0.01$) were measured after equilibration (annealing) at respective T for 15 min. The moduli thus obtained are shown in Figure 2. For clarity of the figure, the moduli are shown only at representative T.

As noted in Figure 2, G' at low ω (<1 s^{-1}) decreases, and its ω dependence is enhanced while G'' at those ω increases with a small increase of T from 25 to 28 °C. Namely, the equilibrium elasticity of the 28 wt % BS/DBP system is largely reduced (or almost vanishes) at 28 °C. At higher T (≥ 31 °C), G' and G'' exhibit the terminal tail, and the system behaves as a viscoelastic fluid having no equilibrium elasticity. For SB micelles

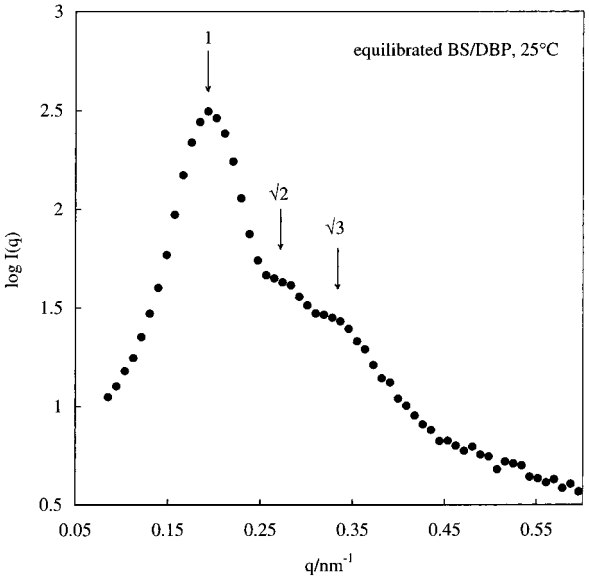

Figure 3. SANS profile of the 28 wt % BS/DBP system quiescently equilibrated at 25 °C. The scattering peak/shoulders shown with the arrows are indicative of a (polycrystalline) bcc lattice of the BS micelles.

in tetradecane, very similar viscoelastic changes result from the micellar lattice disordering (at low T) and S/B mixing (at high T).[13,19] Thus, the changes seen in Figure 2 strongly suggest that the BS/DBP micellar lattice is disordered (but the micelles themselves are preserved) at $T \cong 28$ °C and the B/S mixing occurs at $T > 31$ °C. (T_{MPS} of the 28 wt % system was between 31 and 58 °C, as explained later for Figure 4.)

Thus, the micellar lattice in the 28 wt % BS/DBP system at 25 °C is disordered on slight dilution (from 28 wt % to 25 wt %) and/or slight heating (from 25 °C to 28 °C). This fact suggests that the lattice in this system is not very stable and thus susceptive to mechanical disturbance. Considering this feature, we choose the 28 wt % BS/DBP system at 25 °C as a model system for our tests of the nonlinear shear effects for the micellar lattice. The equilibrium lattice structure in this system is characterized below.

3-1-2. Equilibrium Lattice Structure in 28 wt % BS/DBP System at 25 °C. Figure 3 shows the SANS profile of the 28 wt % BS/DBP system cooled from 60 °C and quiescently equilibrated at 25 °C for 12 h. The two-dimensional profile was azimuthally symmetric, and the circularly averaged scattering intensity, $I(q)$, is plotted against the scattering vector q.

Micelles with B cores and S corona are formed in the BS/DBP system at 25 °C. In Figure 3, the first-order scattering peak and higher order shoulders are observed at $q = 0.19$, 0.27, 0.33 nm^{-1}. The ratio of these q values is very close to $1{:}\sqrt{2}{:}\sqrt{3}$; see the arrows. Thus, an unoriented bcc polycrystalline lattice of the micelles (with the nearest neighbor distance $D \cong 41$ nm) is formed in the equilibrated system.[28] From the bcc cell edge length $a = 2D/\sqrt{3} \cong 47$ nm and the BS concentration, the number of the BS copolymer chains per micelle is calculated to be $n \cong 130$. From this n, the B core radius is evaluated to be $r_{core} \cong 9.1$ nm (under assumption of no swelling of the B cores with DBP). The thickness of the S corona, estimated as the unperturbed rms end-to-end distance $R_{\theta,S}$ of the S block ($R_{\theta,S}$/nm $= 7.27 \times 10^{-2} M_S^{1/2}$)[29] corrected for the repulsion from the B core, is $t_{corona} = \sqrt{2} R_{\theta,S} \cong 23.9$ nm.[30] A correction

factor for a chain tethered on an impenetrable plane,[31] $\sqrt{2}$, has been utilized in this t_{corona} because r_{core} and $R_{\theta,S}$ are comparable in magnitude. Thus, the micelle radius, $R_m = r_{core} + t_{corona} \cong 33$ nm, is significantly larger than $D/2$, meaning that the S corona blocks of neighboring micelles are deeply overlapping with each other. This deep overlapping is concluded even from comparison of an uncorrected R_m ($= r_{core} + R_{\theta,S} \cong 26$ nm) and D/2.

The elastic behavior of the 28 wt % BS/DBP system at 25 °C (Figures 1 and 2) results from this micellar lattice structure. The equilibrium modulus, $G_e = 1.4 \times 10^3$ Pa (evaluated as G' at $\omega = 10^{-2}$ s^{-1}), reflects the thermodynamic stability of the lattice sustained by the deeply overlapping corona S blocks.

In relation to this lattice stability, we need to add a comment for the "softness" of the B cores. The BS concentration, $c_{BS} = 28$ wt %, is just above the lattice formation concentration at 25 °C (cf. Figure 1), despite the deep overlapping of the S corona blocks. In contrast, the lattice of SB micelles having glassy S cores in tetradecane is formed at low c being close to an overlapping threshold of the micelles.[14,19] Thus, our BS micellar lattice is considerably less stable than expected from the deep overlapping of the S corona, and this instability quite possibly results from a large mobility of the B−S junction in a diffuse core/corona interface.[14,19] This result strongly suggests that our B cores and S corona segregate just moderately to give this diffuse interface. This argument is reasonable because our S and B blocks are relatively short and DBP is not extremely S-selective. In fact, Lodge et al.[22,23] examined structures and rheological properties of SI and SIS copolymers (chemically similar to our BS copolymer) in DBP and found that DBP is just moderately selective to S blocks even at low T where the microdomains are formed.

Because of this moderate segregation of the B and S blocks, the spherical B cores of our BS micelles can readily deform under applied strain/stress to allow an increase of the S/B interfacial area. In addition, the B cores are in a liquid state so that they can quickly respond to the applied strain/stress. Thus, the B cores are soft in both thermodynamic and mechanical senses. This "softness" of the B cores becomes a key in our later discussion of the nonlinear shear effects for the BS micellar lattice.

3-1-3. Ultra-slow Dynamics in Micellar Lattice: The micellar lattice is formed in the 28 wt % BS/DBP system at 25 °C (cf. Figure 3). Nevertheless, this system is not purely elastic at low ω, as noted from the increase of G'' with decreasing $\omega < 0.1$ s^{-1} (cf. filled circles in Figures 1 and 2). This increase of G'' may be related to a very slow (partial) relaxation that could occur through several mechanisms, e.g., motion of defects in the micellar lattice[24,32] and/or exchange of BS chains among the micelles. (Because of the "softness" of the B cores, this exchange can certainly occur in a sufficiently long time scale of the full thermal equilibration.)

We also note the other interesting possibility that the above increase of G'' is related to "aging" of so-called soft glassy materials[33,34] such as concentrated emulsions. These materials have an infinitely broad distribution of free energy minima for spatial packing of constituent elements, and the packing state gradually shifts with time to a state of lower free energy. This shift, the aging, proceeds forever because of the broad distribution of free energy minima and could result in a power-law type increase of G'' ($\propto \omega^{-\alpha}$; $0 < \alpha < 1$).[33] In the polycrystalline micellar lattice, the aging may occur through rearrangement of grains.

It is interesting to examine the ultra-slow dynamics that results in the above increase of G'' of our BS micellar lattice. However, this dynamics is out of the main focus of this paper, the nonlinear shear effects for the soft micellar lattice, and considered as a subject of our future work.

The shear-disrupted lattice exhibits rather fast relaxation at $\omega > 0.1$ s^{-1} (cf. Figure 12 shown later). At those ω, the ultra-slow dynamics in the quiescently equilibrated lattice does not emerge (cf. Figures 1 and 2), and this lattice can be simply regarded as an elastic structure.

3-1-4. Relaxation Mechanisms in Systems without Micellar Lattice. The micellar lattice in the 28 wt % BS/DBP system is disordered to exhibit the terminal relaxation at $T \geq 31$ °C; see Figure 2. Although the main focus of this paper is placed on the nonlinear shear effects for the lattice, the dynamics in the shear-disrupted lattice at 25 °C can be intimately related to the equilibrium relaxation mechanism at higher T (≥ 31 °C). From this point of view, the high-T relaxation mechanism(s) is discussed below.

In general, several relaxation mechanisms are available for block copolymers:[32] For our BS/DBP system forming no micellar lattice at $T \geq 31$ °C, the possible mechanisms are (a) orientational relaxation of individual BS chains,[16] (b) relaxation of interface between S corona and B core,[32] (c) diffusion of individual micelles,[16,19,20] and (d) B/S concentration fluctuation.[3−5,32] Mechanisms b and c are limited to the segregated state, and mechanisms a and d can work also in the homogeneously mixed state.

For tests of these mechanisms, we evaluated the terminal relaxation time τ and steady-state compliance J from the G' and G'' data of the 28 wt % BS/DBP system at $T \geq 31$ °C

$$\tau = [G'/\omega G'']_{\omega \to 0}, \; J = [G'/G''^2]_{\omega \to 0} \qquad (1)$$

The compliance reflects the terminal relaxation intensity affected by the slow relaxation mode distribution.[26,35] These τ and J data (summarized in Figure 15 in Appendix A) as well as the G' data were utilized to test the validities of the above mechanisms. For the mechanisms a−c, detailed results of the tests are described in Appendices A−C, and a summary is given below.

Our BS chains are not entangled at $c_{BS} = 28$ wt %. Thus, if the B and S blocks are uniformly mixed and the observed terminal relaxation occurs through mechanism a, the J data of this system should be close to the compliance J_{free} of nonentangled, free (untethered) homopolymers. On the other hand, if the micelles are formed in the system and the system fully relaxes with mechanism a, the J data should be close to the compliance $J_{tethered}$ of nonentangled, tethered homopolymers. Thus, we utilized the Rouse model to evaluate J_{free} ($= 2M_{BS}/5c_{BS}RT$;[26,35] R = gas constant and T = absolute temperature) and $J_{tethered}$ ($= 2M_{BS}/3c_{BS}RT$).[36] Comparing the J data with these J_{free} and $J_{tethered}$ and examining the T dependence of the J and τ data, we found that the 28 wt % BS/DBP system is in the homogeneous state (without significant B/S concentration fluctuation) at $T \geq 58$ °C and the terminal relaxation at those T corre-

sponds to the relaxation of individual BS chains; cf. Appendix A. This result in turn indicates that the microphase separation temperature T_{MPS} of the 28 wt % system is below 58 °C (and thus T_{MPS} < 58 °C also for less concentrated systems).

The above comparison also indicated that the terminal relaxation of the 28 wt % BS/DBP system at T < 58 °C is not attributable to the relaxation of individual chains. We utilized the emulsion models[37−39] to examine whether this low-T relaxation is due to the relaxation of the B/S interface in the micelles (mechanism b). The interfacial relaxation time τ_{int} calculated from the models was orders of magnitude smaller than the τ data at T < 58 °C; cf. Appendix B. Thus, the terminal relaxation at these T is not attributed to the B/S interfacial relaxation.

Randomly dispersed Brownian particles exhibit a viscoelastic stress when their spatial distribution is distorted by the applied strain, and this stress relaxes due to the particle diffusion. This type of relaxation is observed for suspensions of silica particles in an isorefractive media[40,41] as well as for SI micelles ($M_S = 13.9 \times 10^3$ and $M_I = 28.8 \times 10^3$) having glassy S cores and being randomly dispersed in a matrix of low-M homopolyisoprene (hI; $M = 4.1 \times 10^3$).[16,19,20] In particular, these SI micelles had the core and micellar radii (r_{core} = 8 nm and R_m = 28 nm)[16] close to those of our BS micelles ($r_{core} \cong 9.1$ nm and $R_m \cong 33$ nm). Thus, we compared the behavior of our BS/DBP system at T < 58 °C with that of the SI micelles to examine if the terminal relaxation of the BS/DBP system resulted from diffusion of the BS micelles (mechanism c). This comparison revealed that τ of the BS/DBP system is smaller than the micellar diffusion time and that the relaxation mode distribution of this system does not obey an universality seen for the SI micelles; cf. Appendix C. These results allow us to rule out a possibility that the terminal relaxation of the 28 wt % BS/DBP system at T < 58 °C is due to the BS micellar diffusion. This was the case also for the 25 wt % system at 25 °C.

Now, we focus our attention on the B/S concentration fluctuation (mechanism d). In block copolymer systems, concentration profile of the constituent blocks fluctuates with time if the temperature is rather close to the microphase separation temperature T_{MPS}.[3−5,32,42] Strain distorts the dynamic concentration pattern to raise the stress, and the fluctuation dynamics erases this distortion and leads to the viscoelastic relaxation. For polyolefine block copolymer (PEP−PEE) melts, Bates et al.[4] found characteristic features of the viscoelastic relaxation time τ_{fluc} and relaxation intensity I_{fluc} for the fluctuation mechanism: I_{fluc} increases as T approaches T_{MPS}, while τ_{fluc} normalized by the relaxation time τ_{chain} of individual chains does not significantly change with T. If these features are observed for our 28 wt % BS/DBP system at T < 58 °C, its terminal relaxation is attributable to the B/S concentration fluctuation.

On the basis of this argument, the $G'(\omega)$ and $G''(\omega)$ data of the 28 wt % BS/DBP system at various T were shifted along the ω axis to be compared with each other. For the data at T = 31−49 °C, we chose the G'' data at 25 °C as a reference and made the shift in a way that G'' for the highest ω (100 s^{-1}) measured at respective T coincides with the reference data. For T = 58−70 °C, the shift was made in the same way except that the shifted G'' data at 49 °C were re-chosen as the reference. (The data at T = 58−70 °C were overshifted with the first choice of the reference.) Since G'' at high ω is insensitive to slow relaxation modes (e.g., the fluctuation mode) and thus dominated by fast modes resulting from the relaxation of individual chains, this shift effectively achieves the above normalization of τ with respect to τ_{chain}. (In fact, our shift is very similar to that made by Bates et al.[4])

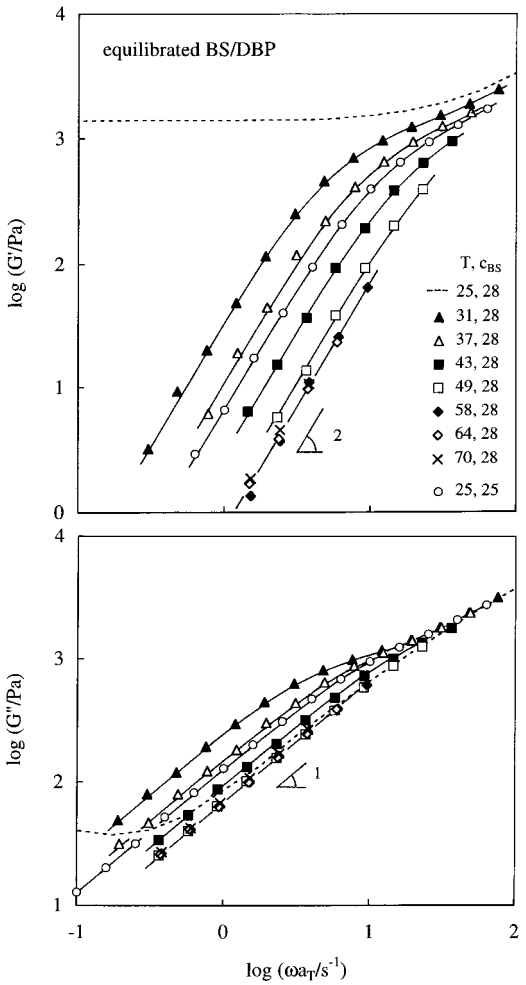

Figure 4. Comparison of the shifted G' and G'' data of the 28 wt % BS/DBP system at various T. The shift along the ω axis was made so as to superpose the $G''(\omega = 100)$ data at respective T onto the reference data. (See text for further details of this shift.) For comparison, the G' and G'' data of the 25 wt % BS/DBP system at 25 °C, shifted in the same way, are also shown (circle).

For the 28 wt % BS/DBP system at various T, the G' and G'' data shifted with the above method are shown in Figure 4 (dotted curves and symbols except the circle). The shift factor a_T is the same for G' and G'' at respective T. Excellent superposition of the data at T = 58−70 °C is achieved with the a_T determined only from the $G''(\omega = 100)$ data at respective T. This thermorheological simplicity is observed because the system at 58−70 °C is in the uniformly mixed state with no significant fluctuation. (Thus, T_{MPS} of this system is between 58 and 31 °C.)

In contrast, with decreasing T < 58 °C, a systematic increase of G' and G'' is noted at ωa_T < 10 s^{-1}. This result demonstrates an increase of the terminal relaxation intensity. We also note that the (shifted) terminal relaxation frequency, $\omega a_T \cong 5$ s^{-1}, does not significantly change with T (<58 °C). Thus, at T = 31−58 °C, the 28 wt % BS/DBP system exhibits the characteristic fea-

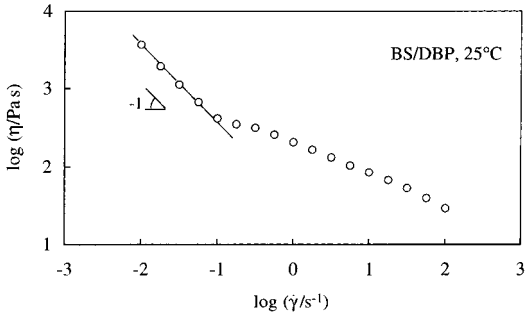

Figure 5. Steady flow behavior of the 28 wt % BS/DBP system at 25 °C.

tures of the B/S concentration fluctuation explained above. (In fact, the changes of G' and G'' with T seen in Figure 4 are similar, in magnitudes, to those observed for PEP-PEE melts.[4]) These results allow us to attribute the terminal relaxation of the 28 wt % BS/DBP system at these T to the fluctuation mechanism.

As a further test of this mechanism, we compared the G' and G'' data of the 25 wt % BS/DBP system at 25 °C with those of the 28 wt % system. For this purpose, we multiplied the data of the former system by a factor of 1.12 (a correction for the small difference of c_{BS} in the two systems) and shifted those corrected data with the above method. The result is shown with the circles in Figure 4. The behavior of the 25 wt % system follows that of the 28 wt % system, and the terminal relaxation frequency ($\omega a_T \cong 5\ s^{-1}$) is nearly the same for these systems. This result demonstrates that the terminal relaxation of the 25 wt % system at 25 °C is also dominated by the B/S concentration fluctuation.

In the model system for our nonlinear shear tests, the 28 wt % BS/DBP system at 25 °C, the lattice is disordered on slight heating and/or slight dilution. This disordered lattice exhibits the terminal relaxation due to the fluctuation mechanism; cf. Figure 4. This fact becomes a key in our later discussion of the nonlinear shear effect for the micellar lattice.

3-2. Nonlinear Shear Effects for Soft Micellar Lattice. 3-2-1. Non-Newtonian Behavior and Structure under Steady Shear. For the 28 wt % BS/DBP system at 25 °C, Figure 5 shows the steady-state shear viscosity η plotted against the shear rate $\dot{\gamma}$. Before the measurements at respective $\dot{\gamma}$, the system was quiescently equilibrated at 25 °C. The η thus measured is proportional to $\dot{\gamma}^{-1}$ and the plastic behavior prevails at $\dot{\gamma} \leq 0.1\ s^{-1}$, while the $\dot{\gamma}$ dependence of η becomes weaker for $\dot{\gamma} > 0.1\ s^{-1}$. The structures corresponding to these non-Newtonian features were detected from SANS measurements under flow, as explained below.

In Figure 6, the SANS profiles of the BS/DBP system under steady shear at representative $\dot{\gamma}$ (curves) are compared with the profile for $\dot{\gamma} = 0$ (quiescently equilibrated state; squares). These profiles are shown in a q range covering the first to third scattering peak/shoulders. The profiles in the low-$\dot{\gamma}$ and high-$\dot{\gamma}$ regimes are presented separately in parts a and b so that their details can be clearly examined. All profiles were obtained with the same SANS exposure time (10 min) and can be compared quantitatively.

As noted in Figure 6a, the width, height, and position (q_1) of the first-order scattering peak hardly change but the higher order shoulders resolved at $\dot{\gamma} = 0$ become a broad tail under slow shear at $\dot{\gamma} = 0.01\ s^{-1}$; cf. thick solid curve. Thus, the long-range order of the BS

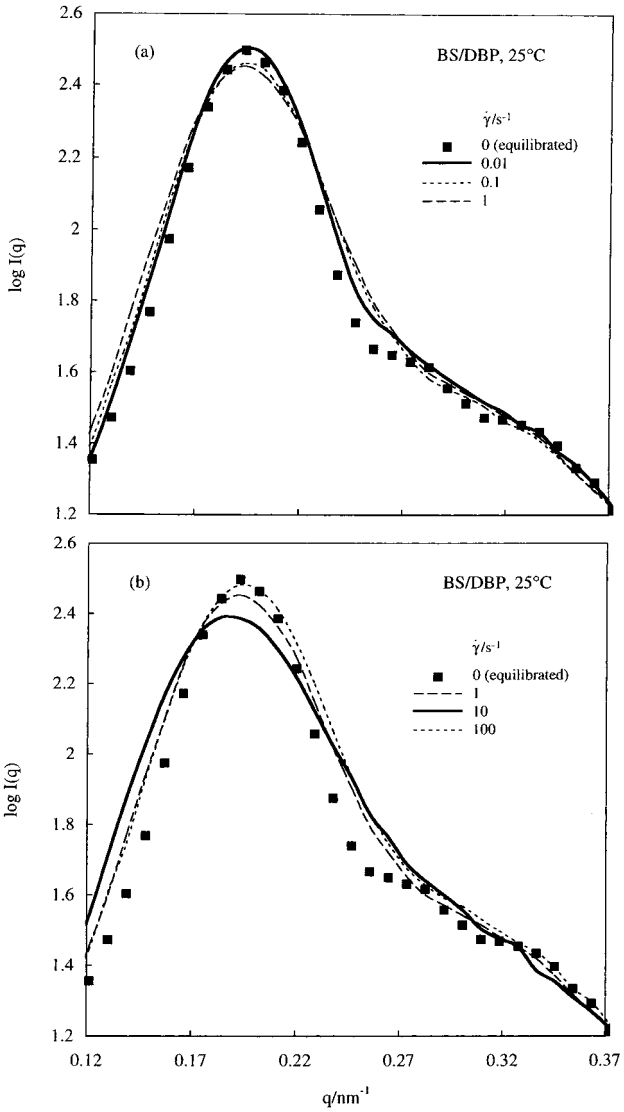

Figure 6. SANS profiles of the 28 wt % BS/DBP system under steady shear at various $\dot{\gamma}$. The profile for $\dot{\gamma} = 0$ (filled squares) was obtained for the quiescently equilibrated system. The profiles in the low-$\dot{\gamma}$ and high-$\dot{\gamma}$ regimes are presented separately in parts a and b so that their details can be easily examined. All profiles were obtained with the same SANS exposure time (10 min) and can be compared quantitatively.

micellar lattice decreases moderately under slow shear. This decrease possibly corresponds to a decrease in the grain size in the polycrystalline bcc lattice, and the flow would occur mainly at intergrain boundaries (at the defects). The plastic behavior (Figure 5) reflects this mild disruption of the lattice.

In Figure 6, the tail (smeared second- and third-order scattering shoulders) does not change much with increasing $\dot{\gamma}$ above $0.1\ s^{-1}$. However, the first-order peak exhibits remarkable changes. This peak becomes broader and lower, but q_1 does not change with increasing $\dot{\gamma}$ from 0.1 to $1\ s^{-1}$; see Figure 6a. Thus, at these $\dot{\gamma}$, the micellar lattice is considerably disrupted but its local order is preserved (as noted from the $\dot{\gamma}$-independence of q_1). Further increase of $\dot{\gamma}$ to $10\ s^{-1}$ results in significant broadening associated with a small decrease of q_1; see Figure 6b. Finally, at $\dot{\gamma} = 100\ s^{-1}$, the peak becomes narrower/higher and q_1 recovers its value for $\dot{\gamma} \leq 1\ s^{-1}$. These results suggest that the lattice is fully disrupted and the micelles are randomly dispersed at $\dot{\gamma} = 10\ s^{-1}$

while the lattice is partly reformed at $\dot{\gamma} = 100\ s^{-1}$. (Since η exhibits no discontinuous change at $\dot{\gamma} = 10\ s^{-1}$ (cf. Figure 5), the BS micelles themselves do not seem to be disrupted even at $\dot{\gamma} = 10\ s^{-1}$.) The non-Newtonian behavior without plastic nature seen at $\dot{\gamma} > 0.1\ s^{-1}$ reflects these structural changes.

Concerning this structure−viscosity relationship of the BS micellar system, we remember that SI micelles having glassy S cores[12,21] as well as colloidal crystals of hard sphere particles[43] exhibit shear-induced lattice melting at high $\dot{\gamma}$. This melting is superficially similar to the full disruption of our BS micellar lattice seen at $\dot{\gamma} = 10\ s^{-1}$. However, the melting of the colloidal crystals results in an increase of η due to hydrodynamic jamming on melting,[43] while no such increase is observed for our BS micellar system. This difference may be partly related to the "softness" of the B cores that allows the core deformation thereby reducing the jamming effect.

It is also known that the colloidal crystals and micellar lattices having rigid cores exhibit the shear-induced orientation at intermediate $\dot{\gamma}$.[10−12,21,43] This orientation never occurred in our BS micellar system, as evidenced from its two-dimensional SANS profile being azimuthally symmetric at all $\dot{\gamma}$ values examined. This lack of the shear-induced orientation is again related to the "softness" of the B cores: The hydrodynamic interaction, that competes with the thermodynamic interaction to induce the lattice orientation, would not be significant in the S/DBP matrix phase between the soft B cores.

3-2-2. Transient Rheological Behavior after Startup of Shear. For the 28 wt % BS/DBP system, Figure 7a shows growth of the shear stress (σ) on startup of the steady shear. The σ data obtained at representative $\dot{\gamma}$ are plotted against the time after the startup. All these data were obtained for the equilibrated system that exhibited the micellar lattice elasticity (cf. Figures 1 and 2) prior to the startup at respective $\dot{\gamma}$.

As seen in Figure 7a, the σ of the equilibrated system exhibits the overshoot before reaching the steady state, and this overshoot becomes less prominent for larger $\dot{\gamma}$. This behavior of our BS/DBP system is essentially different from that of entangled homopolymers: The stress overshoot of these homopolymers is enhanced with increasing $\dot{\gamma}$.[26,35]

The origin of the overshoot of our BS/DBP system is clearly noted in Figure 7b, where unfilled symbols denote the σ data of Figure 7a replotted against the strain, $\gamma = \dot{\gamma}t$. The solid line indicates a stress−strain relationship for the equilibrated micellar lattice, $\sigma = G_e\gamma$, with G_e being the equilibrium modulus of this lattice ($G_e = 1.4 \times 10^3$ Pa; cf. Figures 1 and 2). The σ data for all $\dot{\gamma}$ values grow along this line at small γ, and the overshoot corresponds to the downward deviation from the line. Thus, the overshoot reflects the onset of shear-induced disruption of the lattice. In fact, the behavior before the overshoot is uniquely determined by γ irrespective of the $\dot{\gamma}$ value and coincides with the behavior of the equilibrated lattice.

We also note that the strain at the overshoot increases with increasing $\dot{\gamma}$ (Figure 7b), while the time at the overshoot decreases with $\dot{\gamma}$ (Figure 7a). This result suggests that the lattice disruption requires a characteristic strain as well as a characteristic time. In this sense, the disruption seen here is not a simple, static disruption governed only by the strain.

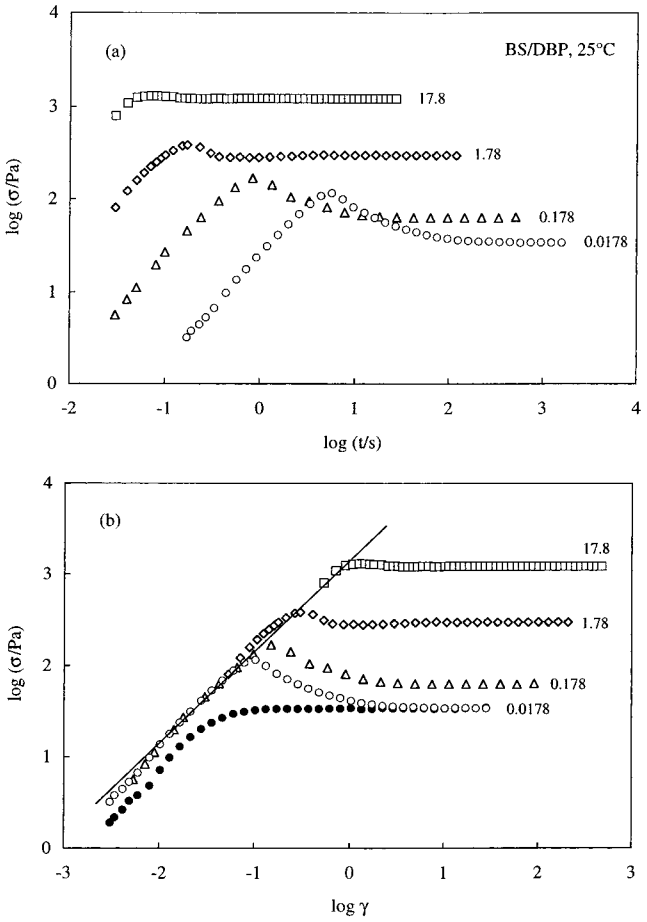

Figure 7. Stress growth of the 28 wt % BS/DBP system on startup of the steady shear. The numbers indicate the shear rate, $\dot{\gamma}/s^{-1}$. In part a, the stress data are plotted against the time t after the startup. These data were obtained for the equilibrated system that exhibited the micellar lattice elasticity prior to the startup at respective $\dot{\gamma}$. In part b, unfilled symbols indicate the data in part a replotted against the strain, $\gamma = \dot{\gamma}t$. The solid line indicates a stress−strain relationship for the equilibrated micellar lattice. Filled circles are the stress data obtained from the second run at $\dot{\gamma} = 0.0178\ s^{-1}$ that was conducted immediately after the first run at the same $\dot{\gamma}$.

In Figure 7, σ exhibits a slow thixotropic decay in particular at low $\dot{\gamma}$. This decay reflects gradual disruption of the lattice with time toward the steadily disrupted state. Once this state is attained, the lattice cannot be reformed immediately after cessation of the shear. This fact can be confirmed from a repeated run of the steady flow experiment made at the same $\dot{\gamma}$ without a resting interval: As shown in Figure 7b, the σ for the second run at $\dot{\gamma} = 0.0178\ s^{-1}$ (filled circles) gradually increases and approaches the steady σ of the first run (unfilled circles). The overshoot is not seen in the second run because the initial and final structures in the second run are identical to the steadily disrupted lattice in the first run and no further disruption occurs in the second run.

3-2-3. Recovery of Lattice Elasticity after Cessation of Shear. For the 28 wt % BS/DBP system presheared at 25 °C, reformation of the micellar lattice required some time. To trace this reformation, we carried out repeated oscillatory tests with a small strain amplitude (0.01) that detected the linear responses of the transient structure during the reformation process without disturbing this structure. This process was

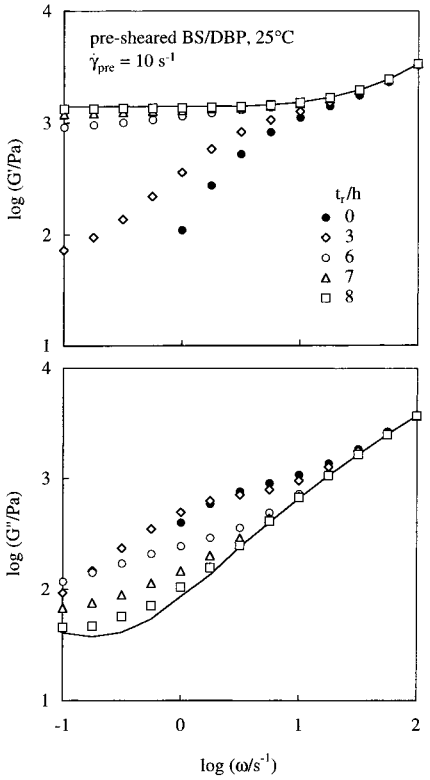

Figure 8. Linear viscoelastic behavior of the 28 wt % BS/DBP system after cessation of the pre-shear at $\dot{\gamma}_{pre} = 10$ s^{-1}. The micellar lattice disrupted under the pre-shear is reformed to various extent according to the time t_r after the pre-shear. The solid curves denote the behavior of the equilibrated micellar lattice.

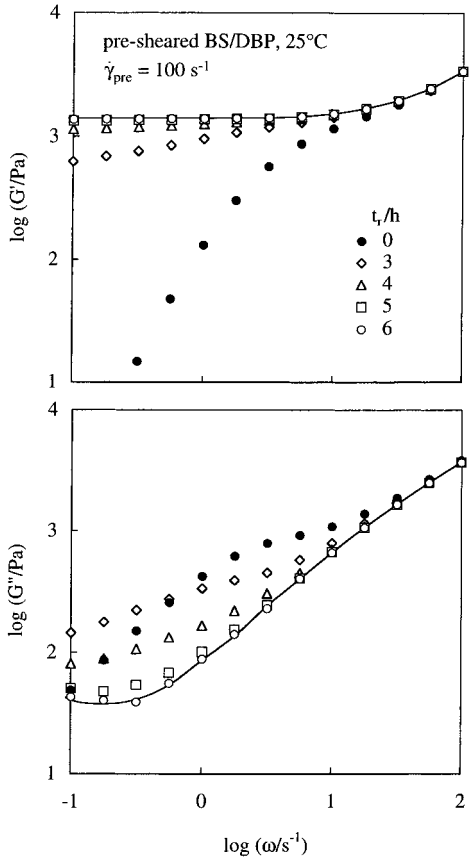

Figure 9. Linear viscoelastic behavior of the 28 wt % BS/DBP system after cessation of the pre-shear at $\dot{\gamma}_{pre} = 100$ s^{-1}. The micellar lattice disrupted under the pre-shear is reformed to various extent according to the time t_r after the pre-shear. The solid curves denote the behavior of the equilibrated micellar lattice.

completed within 8 h, as shown later in Figure 10. Thus, the repeated oscillatory test was made at $\omega \geq 0.1$ s^{-1} so that a time required for each run of the test (≅10 min) was sufficiently shorter than the complete reformation time. The moduli data obtained from this test can be regarded as the isochronal data during the reformation process.

Figures 8 and 9 show typical results of this test for the steady pre-shear at $\dot{\gamma}_{pre} = 10$ and 100 s^{-1}, respectively. In these figures, t_r denotes the time after cessation of the pre-shear, and the solid curves represent the G' and G'' data of the equilibrated BS/DBP system containing the micellar lattice.

In the equilibrated state, individual BS chains relax at high $\omega > 10$ s^{-1}, as explained later for Figure 12. At these ω, the G' and G'' data of the pre-sheared system with various t_r are close to those of the equilibrated BS/DBP system (see Figures 8 and 9), meaning that the relaxation of individual chains is hardly affected by the lattice disruption. More importantly, Figures 8 and 9 demonstrate that the system just after the pre-shear ($t_r = 0$) exhibits the terminal relaxation at $0.1 < \omega/\text{s}^{-1} < 10$. This fact indicates that the lattice disrupted at $\dot{\gamma}_{pre} = 10$ and 100 s^{-1} does not sustain the equilibrium elasticity. The terminal relaxation mechanism of the pre-sheared system is discussed later.

With increasing t_r, the G' and G'' data of the pre-sheared system approach and finally coincide with the data of the equilibrated BS system in the entire range of ω; see Figures 8 and 9. This coincidence, indicating the complete reformation of the micellar lattice, is attained at $t_r \cong 8$ and 5 h for $\dot{\gamma}_{pre} = 10$ and 100 s^{-1}, respectively. Thus, the time t_r^{∞} required for the complete reformation changes with $\dot{\gamma}_{pre}$. (This reformation process as well as the thixotropic disruption process (Figure 7) may be related to the aging[33,34] of the micellar lattice. However, detailed dynamics in these transient processes is beyond the scope of this paper and will be examined in our future work.)

As noted in Figures 8 and 9, the modulus of the equilibrated micellar lattice is recovered in the entire range of ω when G' of the pre-sheared system at $\omega = 0.1$ s^{-1} coincides with G_e of this lattice. Considering this feature, Figure 10 compares this $G'(\omega = 0.1)$ of the pre-sheared system with G_e (horizontal solid line). From the plots shown in Figure 10, t_r^{∞} was evaluated (with an uncertainty of ±30 min) as the t_r for the onset of coincidence of $G'(\omega = 0.1)$ and G_e.

In Figure 11, this t_r^{∞} is plotted against $\dot{\gamma}_{pre}$. We note that t_r^{∞} is the longest for $\dot{\gamma}_{pre} \cong 10$ s^{-1}. This result is consistent with the SANS observation: The reformation is the slowest for the most massively disrupted lattice (for $\dot{\gamma}_{pre} = 10$ s^{-1}; cf. Figure 6).

Now, we may ask a question why the strongest disruption occurred at $\dot{\gamma}_{pre} = 10$ s^{-1}, in other words, why the faster shear ($\dot{\gamma}_{pre} = 100$ s^{-1}) and slower shear ($\dot{\gamma}_{pre} \leq 1$ s^{-1}) resulted in less disruption. To answer this question, we need to know the relaxation mechanism under flow. Our experiments do not resolve this mechanism in situ (i.e., directly under the shear), but useful information can be found from the relaxation behavior of the BS/DBP system just after cessation of the pre-shear (where the disrupted lattice structure under the

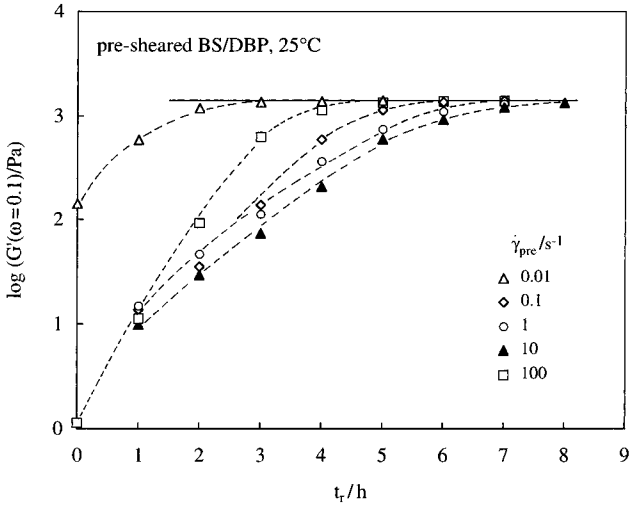

Figure 10. Storage modulus G' at $\omega = 0.1$ s^{-1} obtained for the 28 wt % BS/DBP system after cessation of the pre-shear at various $\dot{\gamma}_{pre}$. The modulus data are plotted against the time t_r after the pre-shear. The horizontal solid line indicates the equilibrium modulus G_e of the fully reformed (equilibrated) micellar lattice.

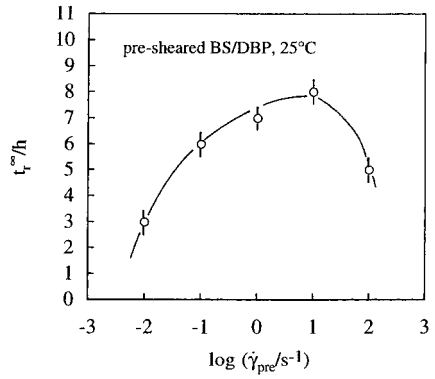

Figure 11. Time t_r^{∞} required for full reformation of the micellar lattice in the 28 wt % BS/DBP system pre-sheared at various $\dot{\gamma}_{pre}$.

pre-shear should be preserved). This behavior is examined below.

3-3. Relaxation Mechanism in Shear-Disrupted Lattice. 3-3-1. Overview. Figure 12 shows the G' (unfilled symbols) and G'' (filled symbols) measured just after cessation of the pre-shear at various $\dot{\gamma}_{pre}$. For clarity of the figure, the data for low $\dot{\gamma}_{pre}$ (≤ 0.1 s^{-1}) and high $\dot{\gamma}_{pre}$ (≥ 1 s^{-1}) are separately presented in parts a and b. We note two separate relaxation processes for all $\dot{\gamma}_{pre}$. The up-turn of the G' and G'' curves seen at $\omega > 10$ s^{-1} is indicative of a fast process, and rapid decreases of G' and G'' at $\omega < 10$ s^{-1} are due to a slow process. The G' and G'' data at $\omega > 10$ s^{-1} do not significantly change with $\dot{\gamma}_{pre}$, suggesting that the fast relaxation mechanism is common in the entire range of $\dot{\gamma}_{pre}$ ($= 0.01-100$ s^{-1}). On the other hand, a significant difference is noted for the slow relaxation mechanism for $\dot{\gamma}_{pre} = 0.01$ s^{-1} and $\dot{\gamma}_{pre} \geq 0.1$ s^{-1}, as explained below.

For $\dot{\gamma}_{pre} = 0.01$ s^{-1}, the BS/DBP system exhibits the slow relaxation characterized with a peak in G'' and a pseudo-plateau of G'. For this relaxation, no terminal tail ($G' \propto \omega^2$ and $G'' \propto \omega$) is detected in our experimental window. In contrast, for $\dot{\gamma}_{pre} \geq 0.1$ s^{-1}, the peak and pseudo-plateau vanish, and the terminal tail is clearly observed. The relaxation rate and intensity characterizing this tail are insensitive to $\dot{\gamma}_{pre}$. In particular, the

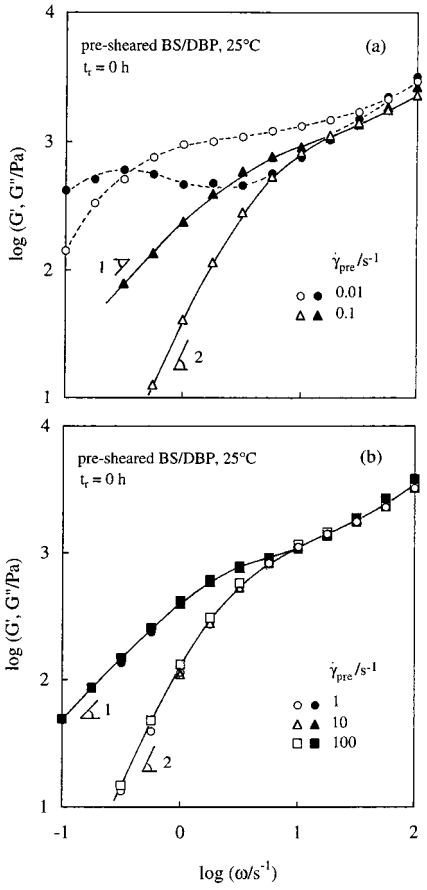

Figure 12. Linear viscoelastic behavior of the 28 wt % BS/DBP system just after cessation of the pre-shear at various $\dot{\gamma}_{pre}$. Unfilled and filled symbols indicate the storage and loss moduli, respectively. For clarity of the figure, the data in the low-$\dot{\gamma}$ and high-$\dot{\gamma}$ regimes are presented separately in parts a and b.

G' and G'' data are almost indistinguishable for $\dot{\gamma}_{pre} \geq 1$ s^{-1}; see Figure 12b. Thus, the terminal relaxation mechanism should be common for $\dot{\gamma}_{pre} \geq 0.1$ s^{-1} but not for $\dot{\gamma}_{pre} = 0.01$ s^{-1}.

3−3−2. Assignment of Terminal Relaxation Mechanism. From the terminal tail of G' and G'' seen for $\dot{\gamma}_{pre} \geq 0.1$ s^{-1} (Figure 12), we evaluated the terminal relaxation time τ and compliance J (cf. eq 1). In Figure 13, these τ and J are plotted against $\dot{\gamma}_{pre}$ (unfilled circles). For $\dot{\gamma}_{pre} = 0.01$ s^{-1}, no terminal tail is observed in our ω window (cf. Figure 12a), and τ and J cannot be determined. However, the other type of average relaxation time τ' can be estimated as a reciprocal of the ω at which the G' and G'' curves cross each other. This τ' is also shown in Figure 13a (filled square).

Analyzing the τ and J data as well as the G' data with the same methods as those applied to the equilibrated systems, we examined validities of several mechanisms for the terminal relaxation in the system pre-sheared at $\dot{\gamma}_{pre} \geq 0.1$ s^{-1}. The results are summarized below.

If the terminal relaxation corresponds to relaxation of individual BS chains, J should be close to J_{free} and/or $J_{tethered}$ of homopolymers estimated from the Rouse model. However, as noted in Figure 13b, the J data (circles) are an order of magnitude larger than J_{free} ($= 2M_{BS}/5c_{BS}RT$; dash−dot line) and $J_{tethered}$ ($= 2M_{BS}/3c_{BS}RT$; dashed line) data. This result indicates that the terminal relaxation of the pre-sheared BS/DBP system is not the relaxation of individual BS chains.

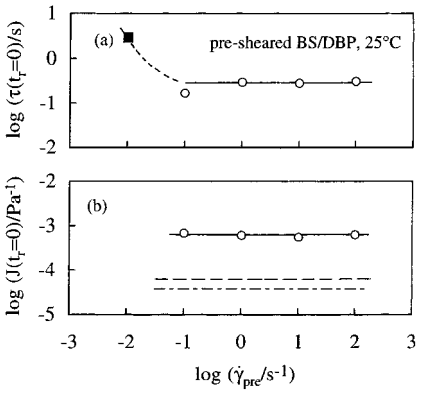

Figure 13. Terminal relaxation time τ (= $[G'/\omega G'']_{\omega\to 0}$) and compliance J of the 28 wt % BS/DBP system just after the pre-shear at various $\dot{\gamma}_{pre}$ (unfilled circles). In part a, the filled square indicates an average relaxation time τ' evaluated from a frequency for cross of the G' and G'' curves. In part b, the dash−dot and dashed lines indicate J_{free} and $J_{tethered}$ of free and tethered Rouse chains having the molecular weight and concentration identical to those of the BS chains.

We also examined if the observed terminal relaxation is due to the B/S interfacial relaxation and/or micellar diffusion. It turned out that the observed relaxation is much slower than the interfacial relaxation (cf. Appendix B), and the G' data do not satisfy the universality seen for the relaxation due to micelle diffusion (cf. Appendix C). Thus, the terminal relaxation of the pre-sheared BS/DBP system is not attributable to those mechanisms.

Now, we test validity of the B/S concentration fluctuation mechanism. Since this mechanism dominates the terminal relaxation in the 28 wt % BS/DBP systems equilibrated at 31 °C (cf. Figure 4), we expect the same situation for the same system pre-sheared at a slightly lower T, 25 °C. Utilizing the method explained for Figure 4, we shifted the G' and G'' data of the pre-sheared system along the ω axis to examine this expectation. These shifted data are shown with the filled symbols in Figure 14. For comparison, the shifted data of the equilibrated system at 31 °C (unfilled diamond) and the reference data at 25 °C (dotted curves) are also shown. (Since the $G''(\omega = 100)$ data of the pre-sheared system were close to but not exactly the same as the reference data, we made a minor shift for this system.)

In the shifted ω-scale of Figure 14, the pre-sheared system at 25 °C exhibits the relaxation similar, in magnitude and frequency, to that of the equilibrated system at 31 °C. This is the behavior expected for the concentration fluctuation process, as explained for Figure 4. In addition, the terminal relaxation time τ of the pre-sheared system at 25 °C was in close agreement with that obtained from short extrapolation of the fluctuation-dominated τ data at T = 31−55 °C; see Figure 15a in Appendix A. From these results, the terminal relaxation in the system pre-sheared at $\dot{\gamma}_{pre} \geq 0.1\ s^{-1}$ is assigned to the B/S concentration fluctuation.[44]

With this assignment for $\dot{\gamma}_{pre} \geq 0.1\ s^{-1}$, we can now specify the mechanism of the terminal relaxation for $\dot{\gamma}_{pre} = 0.01\ s^{-1}$ (Figure 12a). This relaxation is much slower than the relaxation due to the fluctuation seen for $\dot{\gamma}_{pre} \geq 0.1\ s^{-1}$ (cf. Figures 12a and 13a), and the micellar lattice is only mildly disrupted by the pre-shear at $\dot{\gamma}_{pre} = 0.01\ s^{-1}$ (cf. Figure 6). Thus, the terminal relaxation for $\dot{\gamma}_{pre} = 0.01\ s^{-1}$ can be attributed to motion of the

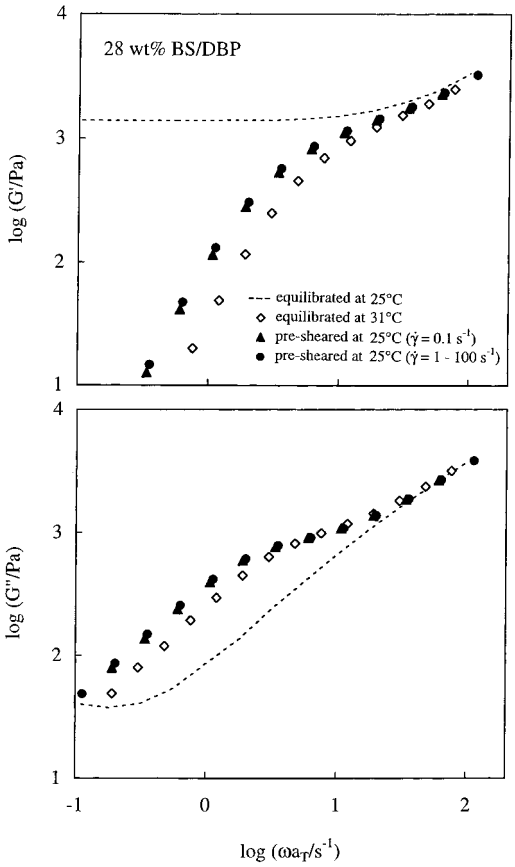

Figure 14. Comparison of the shifted G' and G'' data of the 28 wt % BS/DBP system pre-sheared at 25 °C (filled symbols) with those of the same system equilibrated at 31 °C (unfilled diamond). The shift along the ω axis was made so as to superpose the $G''(\omega = 100)$ data of respective systems onto the reference data (obtained for the system equilibrated at 25 °C; dotted curve). For further details, see text.

micelles in this mildly disrupted lattice: In short time scales, deformation of this lattice under the applied small strain should raise the elasticity similar to that seen for the nondisrupted (equilibrated) lattice. The pseudo-plateau of G' seen for the mildly disrupted lattice (Figure 12a) should reflect this elasticity. However, differing from the situation in the nondisrupted lattice, the micelles would eventually rearrange their positions in the mildly disrupted lattice. This micelle rearrangement possibly results in the observed terminal relaxation. (The characteristic time of the concentration fluctuation in the mildly disrupted lattice would be close to τ for the massively disrupted lattice (unfilled circles in Figure 13a). Thus, in the moderately disrupted lattice, this fluctuation should be completed before the terminal relaxation occurs through the micelle rearrangement.)

3-3-3. Assignment of Fast Relaxation. The above assignments of the terminal relaxation of the pre-sheared system enable us to discuss the mechanism of the fast relaxation seen at $\omega > 10\ s^{-1}$ (Figure 12). This relaxation is common for all $\dot{\gamma}_{pre}$ values, insensitive to the magnitude of the lattice disruption and much faster than the B/S concentration fluctuation (the terminal relaxation seen for $\dot{\gamma}_{pre} \geq 0.1\ s^{-1}$). Thus, the fast relaxation is attributable to the relaxation of individual BS chains. In fact, the chain relaxation followed by a slower concentration fluctuation is observed for many copolymer systems.[4,5,9]

3-4. Role of Concentration Fluctuation in Lattice Disruption. The B/S concentration fluctuation dominates the terminal relaxation of the BS/DBP system just after cessation of the pre-shear at $\dot{\gamma}_{pre} \geq 0.1\ s^{-1}$. The characteristic frequency ω_f of this fluctuation in the quiescent state is evaluated as the reciprocal of the terminal relaxation time, $\omega_f = \tau^{-1} = 3.5 \pm 0.5\ s^{-1}$ (cf. unfilled circles in Figure 13a). The fluctuation should exist also under the steady shear, and its frequency would be close to this ω_f. This fluctuation under shear is the key in our discussion of the lattice disruption.

At low $\dot{\gamma}$, the polycrystalline BS micellar lattice should flow mainly at the intergrain boundaries (defects), and the defect density should increase to reduce the grain size with increasing $\dot{\gamma}$. The B/S concentration fluctuation would tune the number of the BS chains in the shear-created defects (by supplying/removing these chains) to repair these defects. In other words, the fluctuation would tend to preserve the defect density to the equilibrium level. With increasing $\dot{\gamma}$ toward ω_f ($\cong 3.5\ s^{-1}$), this fluctuation becomes overwhelmed by the shear and the defect density should increase accordingly. The gradual disruption of the lattice seen on the increase of $\dot{\gamma}$ up to $1\ s^{-1}$ (Figure 6) seems to result from this competition of the shear and fluctuation.

Here, we note the other, simpler disruption mechanism due to an increase of the shear stress σ with increasing $\dot{\gamma}$. This mechanism may also contribute to the lattice disruption in a range of $\dot{\gamma}$ between 0.1 and $10\ s^{-1}$ where σ ($= \eta\dot{\gamma}$) certainly increases with $\dot{\gamma}$; see Figure 5. However, for lower $\dot{\gamma} \leq 0.1\ s^{-1}$ where the plastic behavior prevails, σ does not increase with $\dot{\gamma}$. The observed enhancement of the lattice disruption in this range of $\dot{\gamma}$ seems to have resulted from the competition of the shear and fluctuation.

Now, we consider the situation in a range of $\dot{\gamma} \gg \omega_f$ where the fluctuation is essentially frozen in the time scale ($\dot{\gamma}^{-1}$) of shear flow. In this time scale, the defects behave as a quenched (nonrepairable), soft structure so that the defect density would be saturated when a continuous defect plane (flow plane) is formed in the direction of shear. In other words, a relatively small amount of defects being oriented in this direction can adsorb the imposed shear, thereby protecting the flowing grains of the lattice. Formation of this defect plane seems to have led to the rather moderate disruption of the lattice at $\dot{\gamma} = 100\ s^{-1} \gg \omega_f$; cf. Figure 6. (At $\dot{\gamma} < \omega_f$, the defect plane should be dynamically undulating due to the concentration fluctuation and not well oriented in the shear direction. Then the lattice is more heavily disrupted with increasing $\dot{\gamma}$ up to ω_f.)

At $\dot{\gamma} \cong \omega_f$, the situation should be between the above two cases. Namely, neither the fluctuation-aided preservation of the defect density nor the quenching of the oriented defect plane (flow plane) effectively works at $\dot{\gamma} \cong \omega_f$. Then the lattice should be most massively disrupted. This seems to be the case for $\dot{\gamma} = 10\ s^{-1}$, the shear rate just above ω_f ($\cong 3.5\ s^{-1}$). In relation to this argument, we should emphasize a fact that the increase of $\dot{\gamma}$ from 10 to $100\ s^{-1}$ leads to the increase of σ ($=\eta\dot{\gamma}$; cf. Figure 5) but allows partial recovery of the lattice order (Figure 6b). This fact, not explained as the mechanical disruption due to the increase of σ, strongly suggests the importance of the oriented defect plane being formed under frozen fluctuation.

The above arguments, explaining why the lattice is most massively disrupted at $\dot{\gamma} = 10\ s^{-1}$, in turn demonstrates the significance of the concentration fluctuation in the nonequilibrium behavior of the BS/DBP system. Although the fluctuation also exists at equilibrium, its contribution to the linear viscoelasticity is overwhelmed by the elasticity of the equilibrated lattice and not well resolved in Figures 1 and 2.

Finally, we should emphasize that the B/S concentration fluctuation results from the thermodynamic/mechanical "softness" of the B cores. This fluctuation is frozen for the previously examined SB micelles having glassy S cores in tetradecane. Thus, the core "softness" is the most prominent feature that distinguishes the BS/DBP micelles from the SB/tetradecane micelles.

4. Concluding Remarks

We have examined rheological and structural properties of a BS diblock copolymer dissolved in a moderately S-selective solvent, DBP. In the well-equilibrated 28 wt % BS/DBP system at 25 °C, spherical micelles with B cores and S corona formed a bcc lattice to exhibit equilibrium elasticity. Under steady shear, this micellar lattice was disrupted to various extent according to the shear rate $\dot{\gamma}$. Mild disruption at low $\dot{\gamma}$ resulted in highly non-Newtonian, plastic flow behavior (associated with thixotropic stress decay in the transient state), and massive disruption at high $\dot{\gamma}$ led to non-Newtonian behavior without plastic nature. The disrupted lattice was spontaneously reformed to recover its equilibrium elasticity during a quiescent rest after cessation of the steady pre-shear. This reformation was the slowest for the most massively disrupted lattice.

Interestingly, the micellar lattice was most massively disrupted under the shear at an intermediate rate, $\dot{\gamma} = 10\ s^{-1}$, not under the faster shear ($\dot{\gamma} = 100\ s^{-1}$) or the slower shear ($\dot{\gamma} = 0.01-1\ s^{-1}$). This behavior can be related to the B/S concentration fluctuation having the characteristic frequency $\omega_f \cong 3.5\ s^{-1}$ in the following way.

Under slow shear at $\dot{\gamma} < \omega_f$, this fluctuation is active and possibly tends to reform the lattice (by tuning the number of the BS chains in the shear-created defect regions). Under fast shear at $\dot{\gamma} \gg \omega_f$, the fluctuation is frozen so that the flow plane (defect plane) oriented in the shear direction is stabilized, thereby allowing the lattice to flow without being subjected to massive disruption. None of these mechanisms effectively works at $\dot{\gamma} = 10\ s^{-1} \cong \omega_f$, quite possibly resulting in the strongest disruption of the lattice at this $\dot{\gamma}$.

It is the softness of the micellar B cores that allows the B/S concentration to fluctuate thereby raising the above effects. This softness is the most prominent feature that distinguishes the BS/DBP micelles from the other micelles having glassy cores and exhibiting no fluctuation.

Acknowledgment. This work was partly supported by Japan Chemical Innovation Institute (through the Doi Project for development of Platform for designing high functional materials). Y.M. acknowledges, with thanks, financial support from a JSPS Research Fellowship for Young Scientist.

Appendix A. Test of Orientation Relaxation of Individual BS Chains

In Figure 15, the terminal relaxation time τ and compliance J of the 28 wt % BS/DBP system equilibrated at $T \geq 31$ °C are plotted against T^{-1} (triangles).

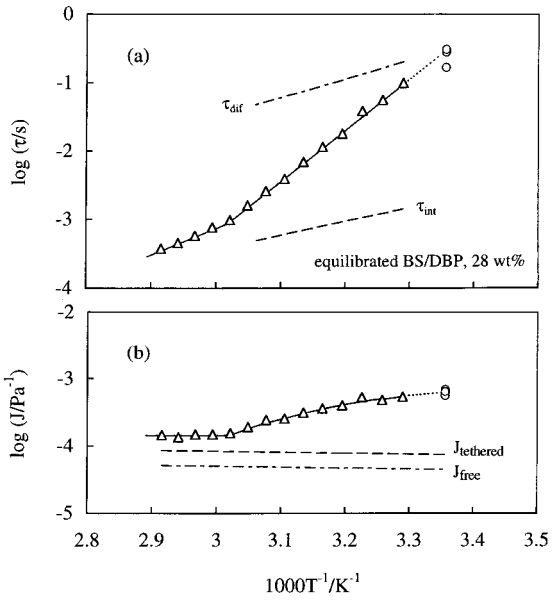

Figure 15. Terminal relaxation time τ and compliance J of the 28 wt % BS/DBP system equilibrated at $T \geq 31$ °C (triangles). Circles indicate the τ and J data of the same system just after the pre-shear at 25 °C.

The circles indicate the τ and J data for the same system just after the pre-shear at 25 °C (cf. Figures 12 and 13).

If the B and S blocks are uniformly mixed and the terminal relaxation of the equilibrated system at $T \geq 31$ °C corresponds to the orientation relaxation of individual, nonentangled BS chains, the J data should be close to the compliance J_{free} of free (untethered) homopolymer chains having the molecular weight M_{BS} and concentration c_{BS}. Experiments established that J_{free} of such nonentangled homopolymers is close to the Rouse compliance[26,35]

$$J_{Rouse} = gM_{BS}/c_{BS}RT \qquad \text{with } g = {}^2/_5 \qquad \text{(A1)}$$

Here, R and T are the gas constant and absolute temperature, respectively, and c_{BS} is the concentration in mass/volume unit.

On the other hand, if the B and S blocks segregate to form micelles and the B−S junctions are localized in the core/corona interface, the J data would be close to $J_{tethered}$ of tethered homopolymer chains. This $J_{tethered}$ can be estimated from eq A1 with $g = 2/3$.[36] (For the segregated BS chains, $J_{tethered}$ may need to be calculated from the c_S and M_S of the corona S block, not from the c_{BS} and M_{BS} utilized in eq A1. However, the $J_{tethered}$ value calculated from c_S and M_S was smaller than that from c_{BS} and M_{BS} only by 6%, and we neglected this small difference.)

The J_{free} and $J_{tethered}$ thus evaluated are shown in Figure 15b with the dash−dot and dashed lines, respectively. The J data at $T \geq 58$ °C ($T^{-1} < 3.03 \times 10^{-3}$ K^{-1}) are quite insensitive to T and agree with J_{free} for the uniform BS chains within a factor of 3. This T-insensitivity indicates that the structure in the 28 wt % BS/DBP system remains the same at those T. In addition, the agreement within a factor of 3, slightly worse compared to the agreement seen for monodisperse homopolymers,[26] can be a natural consequence of a difference in the monomeric friction of the S and B blocks that broadens the relaxation mode distribution[45] to increase J. Thus, at $T \geq 58$ °C, the 28 wt % BS/DBP system is quite possibly in the uniformly mixed state without significant B/S concentration fluctuation, and the terminal relaxation should be dominated by the relaxation of individual BS chains. Consequently, the increase of J ($> J_{free}$) with decreasing $T < 58$ °C suggests that either dynamic or static heterogeneity emerges at these T.

Figure 15b also demonstrates that the J data at $T \geq 58$ °C is closer to the $J_{tethered}$ (for BS micelles; dashed line) than to J_{free}. However, at those T, the J value is insensitive to T, and τ exhibits simple, Ahrrenius-type T dependence (cf. Figure 15a). These results indicate that the structure in the system remains the same in a rather wide range of T between 58 and 70 °C. It is quite unlikely that the micellar structure remains the same in this range of T. For this reason, we can rule out a possibility of the micelle formation at $T \geq 58$ °C.

The micelles may be formed in a range of T between 31 and 55 °C, in particular at low T in this range. However, at these T, the J data are significantly larger than the $J_{tethered}$ data, and the terminal relaxation cannot be assigned as the relaxation of the tethered S and B blocks. This is the case also for the 28 wt % BS/DBP system pre-sheared at 25 °C; see circles in Figure 15b. (The existence of the micelles in the pre-sheared system is confirmed from Figure 6.)

From all above results, we conclude that the orientation relaxation of individual BS chains dominates the terminal relaxation of the 28 wt % BS/DBP system only in the homogeneously mixed state at high $T \geq 58$ °C.

We also made similar analysis for the J data of the BS/DBP systems with $c_{BS} \leq 25$ wt % at 25 °C (cf. Figure 1). For the 20 and 18 wt % systems, J was close to J_{free} and/or $J_{tethered}$, and the observed relaxation was attributable to the relaxation of individual BS chains (probably in the homogeneously mixed state). However, for the 25 wt % system, J was an order of magnitude larger than J_{free} and/or $J_{tethered}$. This result strongly suggests that the micelles are formed in the 25 wt % system but the terminal relaxation does not correspond to the relaxation of the (tethered) BS chains therein.

Appendix B. Test of B/S Interfacial Relaxation

As T is decreased below 58 °C, the J data of the 28 wt % BS/DBP system increase, and the T dependence of τ is enhanced; see Figure 15. These results suggest that the microphase separation temperature T_{MPS} of this system is located between 31 and 58 °C. We can utilize the emulsion models[37−39] to examine if the terminal relaxation in this range of T corresponds to the relaxation of B/S micellar interface. For this purpose, we regarded the B cores as the droplets in emulsions and compared the τ data with the interfacial relaxation time τ_{int} calculated from the models.

This calculation requires us to know the volume fraction ϕ_{core} of the B cores in our BS/DBP system. Under assumption of no volume change on dissolution of BS chains in DBP, we obtained $\phi_{core} \cong 0.059 f_s$, with f_s being the core-swelling ratio. Since DBP is S-selective and the B content in our BS chain is only 20 wt % (Table 1), the micellar B cores formed at $T < T_{MPS}$ have considerably small ϕ_{core}; $\phi_{core} \cong 0.12$ even for a (unrealistically) large swelling ratio, $f_s = 2$. For such small ϕ_{core}, the Choi−Schowalter[37] and Palierne[38] models predict almost identical τ_{int} that can be approximated as the τ_{int} for $\phi_{core} \to 0$

$$\tau_{int} = \frac{\eta_{corona} r_{core}}{40\Gamma} \frac{(19K + 16)(2K + 3)}{K + 1}$$

$$\text{with } K = \frac{\eta_{core}}{\eta_{corona}} \quad (\text{for } \phi_{core} \to 0) \quad \text{(B1)}$$

Here, η_{core} and η_{corona} are the viscosities of the B core and S corona phases (droplet and matrix phases), r_{core} is the B core radius, and Γ is the interfacial tension between the B core and S corona. (In eq B1, we have assumed that the B and S phases behave as Newtonian fluids in the time scale of τ_{int}. This assumption is generally valid in the terminal regime of emulsions.[39])

The r_{core}, η_{core}, and η_{corona} values are required for calculation of τ_{int}. We assumed no core-swelling to utilize the r_{core} value for bulk B cores ($r_{core} = 9.1$ nm). Under the same assumption, we evaluated η_{core} and η_{corona} as

$$\eta_{core} = 3\eta_{hB}, \eta_{corona} = 3\eta_{hS/DBP} \quad \text{(B2)}$$

Here, η_{hB} is a viscosity of bulk, linear homopolybutadiene (hB) having the same M_B as that of the B block, and $\eta_{hS/DBP}$ is a viscosity of a DBP solution of linear homopolystyrene (hS) having the same M_S and c_S as those of the S block. The factor of 3 included in eq B2 accounts for an effect of the tethered ends of the B and S blocks in the BS micelles.[46] The η_{hB} and $\eta_{hS/DBP}$ values were estimated from viscosity data at various T previously obtained for bulk hB[47,48] and hS/DBP solutions[49] of various M and c.

In Figure 15a, the dashed curve indicates the τ_{int} estimated from the above r_{core}, η_B, and η_S values and a typical Γ value, 10^{-3} Nm^{-1}. At $T < 58$ °C, this τ_{int} is orders of magnitude smaller than the observed τ (triangles), and the difference between τ_{int} and τ is well beyond uncertainties in the τ_{int} value (due to the assumption of no core-swelling). This is the case also for the pre-sheared system at 25 °C; see circles. These results allow us to conclude that the terminal relaxation of the (either equilibrated or pre-sheared) 28 wt % BS/DBP system at $T < 58$ °C is not attributed to the B/S interfacial relaxation. From similar comparison of τ and τ_{int}, this conclusion was obtained also for the 25 wt % system at 25 °C.

Appendix C. Test of Relaxation Due to Micellar Diffusion

The previously examined SI micelles ($M_S = 13.9 \times 10^3$ and $M_I = 28.8 \times 10^3$),[16,20] dispersed in a low-M hI matrix ($M = 4.1 \times 10^3$), had the core and micellar radii ($r_{core} = 8$ nm and $R_m = 28$ nm) close to those of our BS micelles. Diffusion measurements[20] revealed that the terminal viscoelastic relaxation time τ of these SI micelles coincides with the time required for the diffusion over the micellar core diameter, $2r_{core}$. Recent analysis[50] demonstrated good agreement between this τ and the Stokes−Einstein diffusion time

$$\tau_{dif} = \frac{\pi R_m (2r_{core})^2 \eta_{eff}}{k_B T} \quad \text{(C1)}$$

where k_B is the Boltzmann constant and η_{eff} is an effective viscosity for the micellar diffusion. For dilute SI micelles, this η_{eff} is close to the matrix viscosity. In contrast, for concentrated SI micelles mutually entangled through their corona, η_{eff} is close to the viscosity associated to the relaxation of individual corona blocks.

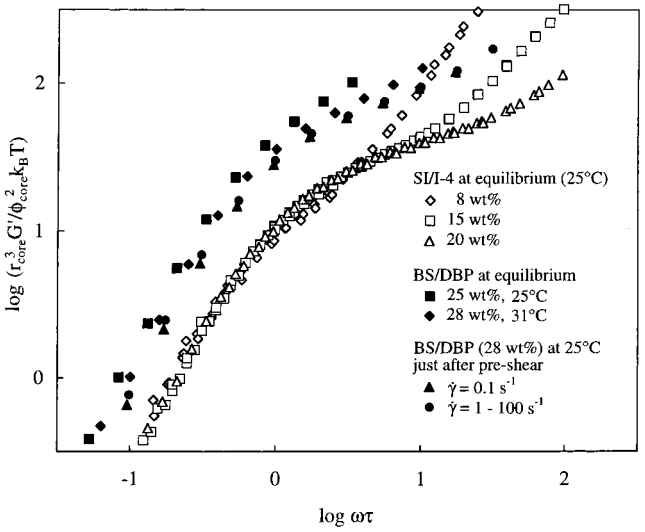

Figure 16. Dependence of reduced modulus of the equilibrated and pre-sheared BS/DBP systems on the normalized frequency $\omega\tau$ (filled symbols). The modulus is indistinguishable for the system pre-sheared at $\dot{\gamma}_{pre} = 1-100$ s^{-1} (filled circle). Unfilled symbols indicate the universal $\omega\tau$ dependence of modulus of previously examined SI micelles (with various c_{SI}).

(Earlier analysis[16,19] indicated that τ is close to a time for diffusion over a distance R_m (eq C1 with $2r_{core}$ being replaced by R_m); however, recent analysis[50] revealed that τ is even closer to τ_{dif} given by eq C1.)

Thus, for our BS micelles being similar in size to the above SI micelles, the viscoelastic τ should be close to τ_{dif} if the terminal relaxation of the 28 wt % BS/DBP system at $T < 58$ °C is dominated by the micellar diffusion. Our BS micelles are not entangled but heavily overlapping with each other. For such concentrated micelles, η_{eff} should not be given by the solvent (DBP) viscosity. Considering this point, we utilized the corona S viscosity η_{corona} obtained under the assumption of no core-swelling (eq B2) as the η_{eff} in eq C1. From this η_{corona} as well as the r_{core} and R_m values obtained under the same assumption, we estimated τ_{dif} of the BS micelles. This τ_{dif} is shown with the dash−dot curve in Figure 15a.

Here, we note that the core-swelling (i.e., extraction of DBP from the S corona phase) increases the η_{eff} (= η_{corona}), r_{core}, and R_m values to increase the τ_{dif} value (cf. eq C1). Thus, the τ_{dif} estimated under the assumption of no core-swelling gives a lower bound for the possible τ_{dif} values. As noted in Figure 15a, even this lower bound is significantly larger than the τ data at $T = 31-55$ °C. This result suggests that the terminal relaxation of the 28 wt % BS/DBP system at these T is not attributable to the micelle diffusion.

For a further test of this diffusion mechanism, we can focus on the relative distribution of the terminal relaxation modes of Brownian suspensions. For Brownian silica particles with the volume fraction $\phi \le 0.5$, Shikata and Perason[40] found that the mode distribution is insensitive to ϕ. This insensitivity leads to universal dependence of a reduced modulus $Q(\phi) r_{core}^3 G'/k_B T$ on a reduced frequency $\omega\tau$,[40] where r_{core} is the particle (hard-core) radius and $Q(\phi)$ is an intensity reduction factor.

For the previously examined SI micelles,[16] we regard here the glassy S cores as the Brownian hard cores and examine whether the above universality holds or not. Since these S cores had a small volume fraction, $\phi_{core} =$

0.023−0.058 for $c_{SI} = 8-20$ wt %, we can utilize the intensity reduction factor $Q(\phi_{core}) = 1/\phi_{core}^2$ (for $\phi_{core} \ll 1$)[40] to examine the universality. In Figure 16, the modulus of the SI micelles reduced by this Q factor is plotted against $\omega\tau$ (unfilled symbols). In the terminal regime at $\omega\tau < 4$, the reduced modulus for $c_{SI} = 8-20$ wt % exhibits the universal $\omega\tau$ dependence, as anticipated. (Deviations from this universality seen at higher $\omega\tau$ reflects the relaxation of individual corona I blocks.[16])

Our BS micelles have the size and ϕ_{core} value similar to those of the above SI micelles. Thus, if the terminal relaxation of the equilibrated BS/DBP system results from diffusion of the BS micelles, its reduced modulus should exhibit the universal $\omega\tau$ dependence. However, for the systems with $c_{BS} = 28$ wt % at 31 °C and with $c_{BS} = 25$ wt % at 25 °C, the modulus (filled square and diamond) exhibits significant upward deviation from the universal curve (unfilled symbols). Thus, the terminal relaxation of these systems is not attributable to the micelle diffusion, confirming the conclusion obtained from the comparison of τ and τ_{dif} (Figure 15a).

Figure 16 also examines the micelle diffusion mechanism for the 28 wt % BS/DBP system pre-sheared at 25 °C ($\dot{\gamma}_{pre} = 0.1-100$ s^{-1}). The reduced modulus of this system (filled triangle and circle) exhibits significant upward deviation from the universal curve, indicating that the micelle diffusion is not the mechanism for the terminal relaxation in the pre-sheared system.

References and Notes

(1) Molau, G. E. Colloidal and Morphological Behavior of Block and Graft Copolymers. In *Block Polymers*; Aggarwal, S. L., Ed.; Plenum Press: New York, 1970.
(2) Sadron, C.; Gallot, B. *Macromol. Chem.* **1973**, *164*, 301.
(3) Bates, F. S.; Fredrickson, G. H. *Annu. Rev. Phys. Chem.* **1990**, *41*, 525.
(4) Bates, F. S.; Rosedale, J. H.; Fredrickson, G. H. *J. Chem. Phys.* **1990**, *92*, 6255.
(5) Koppi, K. A.; Tirrell, M.; Bates, F. S.; Almdal, K.; Colby, R. H. *J. Phys. II (Fr.)* **1992**, *2*, 941.
(6) Larson, R. G.; Winey, K. I.; Patel, S. S.; Watanabe, H.; Bruinsma, R. *Rheol. Acta* **1993**, *32*, 245.
(7) Patel, S. S.; Larson, R. G.; Winey, K. I.; Watanabe, H. *Macromolecules* **1995**, *28*, 4313.
(8) Koppi, K. A.; Tirrell, M.; Bates, F. S.; Almdal, K.; Mortensen, K. *J. Rheol.* **1994**, *38*, 999.
(9) Zhao, J.; Majumdar, B.; Schulz, M. F.; Bates, F. S.; Almdal, K.; Mortensen, K.; Hajduk, D. A.; Gruner, S. M. *Macromolecules* **1996**, *29*, 1204.
(10) Mortensen, K.; Brown, W.; Nordén, B. *Phys. Rev. Lett.* **1992**, *68*, 2340.
(11) Phoon, C. L.; Higgins, J. S.; Allegra, G.; Van Leeuwen, P.; Staples, E. *Proc. Royal Soc. London, Ser. A* **1993**, *442*, 221.
(12) McConnell, G. A.; Lin, M. Y.; Gast, A. P. *Macromolecules* **1995**, *28*, 6754.
(13) Watanabe, H.; Kotaka, T.; Hashimoto, T.; Shibayama, M.; Kawai, H. *J. Rheol.* **1982**, *26*, 153.
(14) Watanabe H.; Kotaka, T. *Polymer J.* **1983**, *15*, 337.
(15) Watanabe H.; Kotaka, T. *J. Rheol.* **1983**, *27*, 223.
(16) Sato, T.; Watanabe, H.; Osaki, K.; Yao, M. L. *Macromolecules* **1996**, *29*, 3881.
(17) Watanabe, H.; Sato, T.; Osaki, K.; Yao, M. L. *Macromolecules* **1996**, *29*, 3890.
(18) Watanabe, H.; Yao, M. L.; Sato, T.; Osaki, K. *Macromolecules* **1997**, *30*, 5905.
(19) Watanabe, H. *Acta Polym.* **1997**, *48*, 215.
(20) Watanabe, H.; Sato, T.; Osaki, K.; Hamersky, M. W.; Chapman, B. R.; Lodge, T. P. *Macromolecules* **1998**, *31*, 3740.
(21) Watanabe, H.; Kanaya, T.; Takahashi, Y. *Macromolecules* **2001**, *34*, 666.
(22) Lodge, T. P.; Xu, X.; Ryu, C. Y.; Hamley, I. W.; Fairclough, J. P. A.; Ryan, A. J.; Pedersen, J. S. *Macromolecules* **1996**, *29*, 5955.
(23) Hanley, K. J.; Lodge, T. P.; Huang, C. I. *Macromolecules* **2000**, *33*, 5918.
(24) Kossuth, M. B.; Morse, D. C.; Bates, F. S. *J. Rheol.* **1999**, *43*, 167.
(25) Watanabe, H.; Urakawa, O.; Kotaka, T. *Macromolecules* **1994**, *27*, 3525.
(26) Ferry, J. D. *Viscoelastic Properties of Polymers*, 3rd ed.: Wiley: New York, 1980.
(27) Takahashi, Y.; Noda, M.; Naruse, M.; Kanaya, T.; Watanabe, H.; Kato, T.; Imai, M.; Matsushita, Y. *J. Soc. Rheol. Jpn.* **2000**, *28*, 187.
(28) The positions of the scattering peak/shoulders, $q_1:q_2:q_3 = 0.19:0.27:0.33 \cong 1:\sqrt{2}:\sqrt{3}$, are consistent also with the simple cubic (sc) lattice with $D \cong 33$ nm and $r_{core} \cong 8.1$ nm. However, this r_{core} value is somewhat smaller than the unperturbed dimension of the B block ($R_{\theta,B} \cong 9.7$ nm), suggesting that the micellar lattice in our BS/DBP system is more likely to be the bcc lattice (with $D \cong 41$ nm and $r_{core} \cong 9.1$ nm $\cong R_{\theta,B}$). Note also that the deep overlapping of the neighboring micelles (i.e., R_m (= $r_{core} + t_{corona}$) being considerably larger than D/2) is concluded even if our micellar lattice is of the sc type.
(29) Miyaki, Y.; Einaga, Y.; Fujita, H. *Macromolecules* **1978**, *11*, 1180.
(30) Strong expansion of S chains due to the excluded volume interaction in good solvents is observed only for $M_S > 10^5$, as noted from the data by Miyaki et al.[29] Thus, our short S block ($M_S = 53.9 \times 10^3$) should exhibit no significant expansion in DBP.
(31) Dimarzio, E. A. *J. Chem. Phys.* **1965**, *42*, 2101.
(32) Watanabe, H. *Rheology of Multiphase Polymeric Systems*. In *Structure and Properties of Multiphase Polymeric Materials*; Araki, T., Qui, T. C., Shibayama, M., Eds.; Marcel Dekker: New York, 1998; Chapter 9.
(33) Fielding, S. M.; Sollich, P.; Cates, M. E. *J. Rheol.* **2000**, *44*, 323.
(34) Cloitre, M.; Borrega, R.; Leibler, L. *Phys. Rev. Lett.* **2000**, *85*, 4819.
(35) Watanabe, H. *Prog. Polym. Sci.* **1999**, *24*, 1253.
(36) From the relaxation modulus of tethered Rouse chains,[36b] $G(t) = (cRT/M)\,\Sigma_{p=odd} \exp(-tp^2/\tau_1)$, with τ_1 = longest relaxation time, we obtain $J_{tethered} = (M/cRT)\,\Sigma_{p=odd}\, p^{-4}/\{\Sigma_{p=odd} p^{-2}\}^2 = 2M/3cRT$. (b) Graessley, W. W. *Adv. Polym. Sci.* **1982**, *47*, 67.
(37) Choi, S. J.; Schowalter, W. R. *Phys. Fluid* **1975**, *18*, 420.
(38) Palierne, J. F. *Rheol. Acta* **1990**, *29*, 204.
(39) Graebling, D.; Muller, R.; Palierne, J. F. *Macromolecules* **1993**, *26*, 320.
(40) Shikata, T.; Pearson. D. S. *J. Rheol.* **1994**, *38*, 601.
(41) Watanabe, H.; Yao, M. L.; Yamagishi, A.; Osaki, K.; Shikata, T.; Niwa, H.; Morishima, Y. *Rheol. Acta* **1996**, *35*, 433.
(42) Fredrickson, G. H.; Helfand, E. *J. Chem. Phys.* **1988**, *89*, 5890.
(43) Chen, L. B.; Chow, M. K.; Ackerson, B. J.; Zukoski, C. F. *Langmuir* **1994**, *10*, 2817.
(44) The micellar lattice in the 28 wt % BS/DBP system at 25 °C is disrupted to various extent under the pre-shear at various $\dot{\gamma}_{pre}$; cf. Figure 6. Nevertheless, the relaxation behavior the of the pre-sheared system is insensitive to the $\dot{\gamma}_{pre}$ value in the range between 0.1 and 100 s^{-1}; cf. Figures 12 and 13. This result suggests that the fluctuation dynamics dominating this relaxation is not sensitive to the degree of lattice disruption attained in this $\dot{\gamma}_{pre}$ range.
(45) Yao, M. L.; Watanabe, H.; Adachi, K.; Kotaka T. *Macromolecules* **1992**, *25*, 1699.
(46) The viscosity of free Rouse chains is given by $\eta_{free} = \pi^2 M\tau_1/6cRT$, with τ_1 being the longest relaxation time.[35] Tethered Rouse chains of the same M and c have the longest relaxation time $\tau_1' = 4\tau_1$, and their viscosity is written as $\eta_{tethered} = \pi^2 M\tau_1'/8cRT = 3\eta_{free}$. The resulting ratio, $\eta_{tethered}/\eta_{free} = 3$, was utilized in eq B2 as a factor accounting for the effect of tethered ends.
(47) Colby, R. H.; Fetters, L. J.; Graessley, W. W. *Macromolecules* **1987**, *20*, 2226.
(48) Watanabe, H.; Urakawa, O.; Yamada, H.; Kotaka, T. *Macromolecules* **1996**, *29*, 755.
(49) Watanabe, H.; Kotaka, T. *Macromolecules* **1986**, *19*, 2520.
(50) Watanabe, H. *Kobunshi Ronbunshu* **2001**, *58*, 135.

MA0105587